

Signal Transduction:
The Scaffold Protein Shoc2/SUR-8
Accelerates the Interaction of Ras and Raf

SIGNAL TRANSDUCTION



Rie Matsunaga-Udagawa, Yoshihisa Fujita,
Sayaka Yoshiki, Kenta Terai, Yuji Kamioka,
Etsuko Kiyokawa, Katsuyuki Yugi, Kazuhiro
Aoki and Michiyuki Matsuda

J. Biol. Chem. 2010, 285:7818-7826.

doi: 10.1074/jbc.M109.053975 originally published online January 5, 2010

Access the most updated version of this article at doi: [10.1074/jbc.M109.053975](https://doi.org/10.1074/jbc.M109.053975)

Find articles, minireviews, Reflections and Classics on similar topics on the [JBC Affinity Sites](#).

Alerts:

- [When this article is cited](#)
- [When a correction for this article is posted](#)

[Click here](#) to choose from all of JBC's e-mail alerts

Supplemental material:

<http://www.jbc.org/content/suppl/2010/01/05/M109.053975.DC1.html>

This article cites 40 references, 15 of which can be accessed free at
<http://www.jbc.org/content/285/10/7818.full.html#ref-list-1>

The Scaffold Protein Shoc2/SUR-8 Accelerates the Interaction of Ras and Raf^{*[5]}

Received for publication, August 9, 2009, and in revised form, December 19, 2009. Published, JBC Papers in Press, January 5, 2010, DOI 10.1074/jbc.M109.053975

Rie Matsunaga-Udagawa⁺¹, Yoshihisa Fujita⁺¹, Sayaka Yoshiki[‡], Kenta Terai⁺², Yuji Kamioka[§], Etsuko Kiyokawa[§], Katsuyuki Yugi[¶], Kazuhiro Aoki^{¶||3}, and Michiyuki Matsuda^{+§}

From the [‡]Laboratory of Bioimaging and Cell Signaling, Graduate School of Biostudies, and the [§]Department of Pathology and Biology of Diseases, Graduate School of Medicine, Kyoto University, Kyoto 606-8501, the [¶]Department of Biosciences and Informatics, Keio University, Kanagawa 223-8522, and ^{||}PREST, Japan Science and Technology Agency (JST), 4-1-8 Honcho, Kawaguchi, Saitama 332-0012, Japan

Shoc2/SUR-8 positively regulates Ras/ERK MAP kinase signaling by serving as a scaffold for Ras and Raf. Here, we examined the role of Shoc2 in the spatio-temporal regulation of Ras by using a fluorescence resonance energy transfer (FRET)-based biosensor, together with computational modeling. In epidermal growth factor-stimulated HeLa cells, RNA-mediated Shoc2 knockdown reduced the phosphorylation of MEK and ERK with half-maximal inhibition, but not the activation of Ras. For the live monitoring of Ras binding to Raf, we utilized a FRET biosensor wherein Ras and the Ras-binding domain of Raf were connected tandemly and sandwiched with acceptor and donor fluorescent proteins for the FRET measurement. With this biosensor, we found that Shoc2 was required for the rapid interaction of Ras with Raf upon epidermal growth factor stimulation. To decipher the molecular mechanisms underlying the kinetics, we developed two computational models that might account for the action of Shoc2 in the Ras-ERK signaling. One of these models, the Shoc2 accelerator model, provided a reasonable explanation of the experimental observations. In this Shoc2 accelerator model, Shoc2 accelerated both the association and dissociation of Ras-Raf interaction. We propose that Shoc2 regulates the spatio-temporal patterns of the Ras-ERK signaling pathway primarily by accelerating the Ras-Raf interaction.

The Ras/Raf/mitogen-activated protein kinase kinase (MEK)⁴/extracellular signal-regulated kinase (ERK) kinase cas-

cade, simply called the Ras-ERK signaling cascade hereafter, plays important roles in proliferation, differentiation, apoptosis, and oncogenic transformation (1–5). The activity of the small GTPase Ras is spatially and temporally regulated by two classes of proteins, guanine nucleotide exchange factor (GEF) and GTPase-activating protein (GAP) (6–9). GEF promotes the exchange of GDP for GTP of Ras, yielding the GTP-bound active Ras (Ras-GTP). On the other hand, GAP stimulates the intrinsic GTPase activity of Ras, thereby restoring the GDP-bound inactive state (Ras-GDP). Both GEFs and GAPs are regulated by kinases, phosphatases, calcium ions, phospholipids, etc.; therefore, Ras serves as the sensor or input device in the Ras-ERK signaling cascade. Activated Ras-GTP then directly binds to and activates Raf, which triggers sequential activation of MEK, a MAP kinase kinase, and ERK. ERK, which is the effector or output device of this signaling cascade, in turn phosphorylates and activates/inactivates many proteins, disseminating signals within the cells.

In addition to the aforementioned components, scaffold proteins, which bind two or more of the components and thereby provide platforms for signaling, have been shown to regulate the Ras-ERK signaling cascade in many ways (10, 11). Computational modeling and engineered scaffold proteins have greatly helped us to understand such functions of scaffold proteins (12, 13). These proteins regulate the Ras-ERK signaling cascade in several ways: first, by providing platforms on which signaling molecules can be efficiently assembled; second, by localizing signaling molecules at specific sites within a cell; third, by coordinating positive and negative feedback signals to tune the signaling strength; and last, by protecting activated signaling molecules from inactivation (10, 11). These functions of scaffold proteins add additional complexity to the Ras-ERK signaling cascade, allowing such variations as graded *versus* digital signaling, and transient *versus* sustained *versus* oscillatory signaling (12). Several scaffold proteins that assemble the components of this Ras-ERK signaling cascade have been identified by genetic screens in *Drosophila melanogaster* and *Caenorhabditis elegans* (14). Examples include the kinase suppressor of Ras, MEK partner 1, connector enhancer of kinase suppressor of Ras, and soc-2 suppressor of clear homolog (Shoc2).

yellow fluorescent protein; siRNA, small interfering RNA; EGFP, enhanced green fluorescent protein; TFP, teal fluorescent protein.

* This work was supported by a Grant-in-aid for Scientific Research on Priority Areas from the Ministry of Education, Culture, Sports, and Science of Japan, a Sagawa Cancer Research Grant, the Japan Science and Technology PRESTO program, and funds from the Kyoto University Global COE program, "Center for Frontier Medicine."

[5] The on-line version of this article (available at <http://www.jbc.org>) contains supplemental Figs. S1–S2 and Tables S1–S2.

¹ Both authors contributed equally to this work.

² Present address: Dept. of Biochemistry and Molecular Genetics, University of Virginia, School of Medicine, Charlottesville, VA 22908.

³ To whom correspondence should be addressed: Laboratory of Bioimaging and Cell Signaling, Graduate School of Biostudies, Kyoto University, Kyoto 606-8501, Japan. Tel.: 81-75-753-9450; Fax: 81-75-753-4698; E-mail: k-aoki@lif.kyoto-u.ac.jp.

⁴ The abbreviations used are: MEK, mitogen-activated protein kinase kinase; ERK, extracellular signal-regulated kinase; GEF, guanine nucleotide exchange factor; GAP, GTPase-activating protein; Shoc2, soc-2 suppressor of clear homolog; FRET, fluorescence resonance energy transfer; EGF, epidermal growth factor; AF, acceleration factor; MAP, mitogen-activated protein; GST, glutathione S-transferase; CFP, cyan fluorescent protein; YFP,

The Shoc2 protein, also known as a suppressor of Ras-8 (SUR-8), is found in all multicellular organisms, suggesting its pivotal role in the Ras/ERK MAP kinase cascade (15, 16). By yeast two-hybrid analysis, Shoc2 has been shown to interact with Ras but not with other Ras family GTPases (17). Shoc2 has also been found to form a complex with Raf-1 in mammalian cells and to enhance the signaling strength of Ras by promoting the Ras-Raf interaction (17). It has been reported that Erbin, a member of the leucine-rich repeat and PDZ domain family, inhibits the interaction of Shoc2 with Ras and Raf and thereby inhibits the Ras/ERK MAP kinase cascade, suggesting that the binding of Ras and Raf to the Shoc2 scaffold protein is also subject to regulation (18). More recently, Shoc2 in a phosphatase holoenzyme complex has been shown to bind to M-Ras and thereby activate Raf proteins by means of the dephosphorylation of 14-3-3 binding sites (19). Thus, it remains a matter of controversy how Shoc2 regulates the signaling from Ras to Raf.

Fluorescence resonance energy transfer (FRET) is a quantum-mechanical phenomenon that occurs between two fluorophores (20, 21). By using probes based on the principle of FRET, several components of the oncogene signaling cascade have been visualized in a living cell (22). Meanwhile, computational simulation has also emerged as a powerful tool for dissecting complex networks of signaling pathways (23, 24). Here we have attempted to clarify the role of Shoc2 in the Ras-ERK signaling cascade with FRET imaging and computational modeling. Our results show that the signaling step from Ras to Raf functions as a low-pass filter without Shoc2. Thus, Shoc2 is essential to transmit the Ras signal to ERK without delay.

EXPERIMENTAL PROCEDURES

FRET Biosensor and Plasmids—pRaichu-Ras consists of mYFP, K-Ras (amino acids 1–172), the Ras-binding domain of c-Raf (amino acids 51–131), mCFP, and the COOH-terminal hypervariable region of K-Ras (amino acids 169–188) from the amino terminus (25). For the purpose of establishing a stable cell line expressing Raichu-Ras, the mCFP was substituted with monomerized teal fluorescent protein (mTFP) (26). The essential properties of the modified Raichu-Ras were the same as those of the original Raichu-Ras (data not shown). The reasons we chose TFP instead of CFP were, first, recombination of CFP and YFP was inevitable when the prototype Raichu-Ras was introduced into the target cells, and, second, mTFP is brighter than CFP and is probably a better donor, as reported previously (27). The cDNA of Raichu-Ras was inserted into pCX4bsr (28) to generate pCX4bsr-Raichu-Ras. The cDNA of Shoc2 was subcloned into the pIRM21-FLAG and pCXN2-GST expression vectors (29, 30) to generate pIRM21-FLAG-Shoc2 and pCXN2-GST-Shoc2, respectively. The cDNA for K-Ras-G12V was inserted into the pCXN2-EGFP expression vector (23) to generate pCXN2-EGFP-K-Ras-V12.

Cells, Reagents, and Antibodies—HeLa cells were purchased from the Human Science Research Resources Bank (Sennan-shi, Japan). The murine ecotropic retrovirus receptor (EcoVR) was first introduced by using the virus produced from BOSC23 cells by transfecting with pCX4hyg-EcoVR, the packaging plasmid pGP, and the envelope plasmid pVSV-G (28). Then, a stable cell line of HeLa cells was generated by infecting HeLa

EcoVR cells with a retrovirus obtained from MSCVpac-eGRF-transfected BOSC23 cells and selection with blasticidin. HeLa cells were maintained in Dulbecco's modified Eagle's medium (Sigma) supplemented with 10% fetal bovine serum. The COS7 cells used in this study were COS7/E3, a subclone of COS7 cells established by Y. Fukui (University of Tokyo, Tokyo, Japan). The cells were maintained in Dulbecco's modified Eagle's medium supplemented with 10% fetal bovine serum. Expression plasmids were transfected into COS7 cells by 293fectin according to the manufacturer's instructions (Invitrogen). Epidermal growth factor (EGF) was purchased from Sigma. Anti-tubulin and anti-pan-Ras (Ab-3) mouse monoclonal antibodies, which recognize H-, K-, and N-Ras, were purchased from Calbiochem (La Jolla, CA). Anti-MEK1/2, anti-ERK1/2, anti-phospho-MEK1/2 (Ser^{217/221}), and anti-phospho-ERK1/2 (Thr²⁰²-Tyr²⁰⁴) were purchased from Cell Signaling Technology (Beverly, MA). Anti-pan-ERK antibody was purchased from BD Transduction Laboratories (San Jose, CA). To obtain the anti-Shoc2 rabbit serum, a polypeptide corresponding to amino acids 70–83 of human Shoc2 was synthesized, bound to Keyhole limpet hemocyanin, and inoculated into rabbits with complete Freund's adjuvant (Covalab, Villeurbanne, France).

RNA Interference Experiments—RNA interference oligomers containing 19 nucleotides were synthesized in the sense and antisense directions with dT-dT overhangs at each 3' terminus. Human Shoc2-targeting siRNAs (5'-AAGCUGCGGAUGCUUGAUUUAdTdT-3') and a scramble control siRNA (5'-CACCUAAUCCGUGGUUCA-3') were synthesized by Gene Design Inc. (Mino-shi, Osaka, Japan). siRNAs were transfected with RNAiMAX (Invitrogen) in HeLa cells according to the manufacturer's instructions. After transfection, cells were incubated for at least 48 h before analysis.

Pull-down Assay—The pull-down assay was performed essentially as described previously (29). HeLa cells were lysed in lysis buffer (50 mM Tris-HCl, pH 7.5, 200 mM NaCl, 2.5 mM MgCl₂, 1% Nonidet P-40, 10% glycerol, 1 mM phenylmethylsulfonyl fluoride, 10 μg/ml of aprotinin, and 10 μg/ml of leupeptin), and clarified by centrifugation. For the measurement of Ras activity, the supernatant was incubated with 10 μg of GST-Raf-RBD fusion proteins. The resulting complexes of GTP-bound Ras and GST-Raf-RBD were precipitated with glutathione-Sepharose beads (Amersham Biosciences) and separated by SDS-PAGE, followed by immunoblotting with anti-Ras antibody. For the detection of binding of Raichu-Ras or EGFP-Ras with Shoc2, GST-Shoc2 in the supernatant was precipitated with glutathione-Sepharose beads, separated by SDS-PAGE, and analyzed by immunoblotting with anti-GST and anti-GFP antibodies.

Time Lapse FRET Imaging—The cells were plated on 35-mm glass-base dishes (Asahi Techno Glass, Tokyo, Japan), which were coated with collagen type I (Nitta Gelatin Inc., Osaka, Japan), and maintained in phenol red-free minimal essential medium prior to imaging (Nissui, Tokyo, Japan). Cells expressing FRET probes were imaged with inverted microscopes (IX71 or IX81; Olympus, Tokyo, Japan) equipped with a Cool SNAP-HQ-cooled charge-coupled device camera (Roper Scientific, Trenton, NJ) controlled with MetaMorph software (Universal Imaging, West Chester, PA) as described previously (25). The

Shoc2 Regulates Ras Signaling

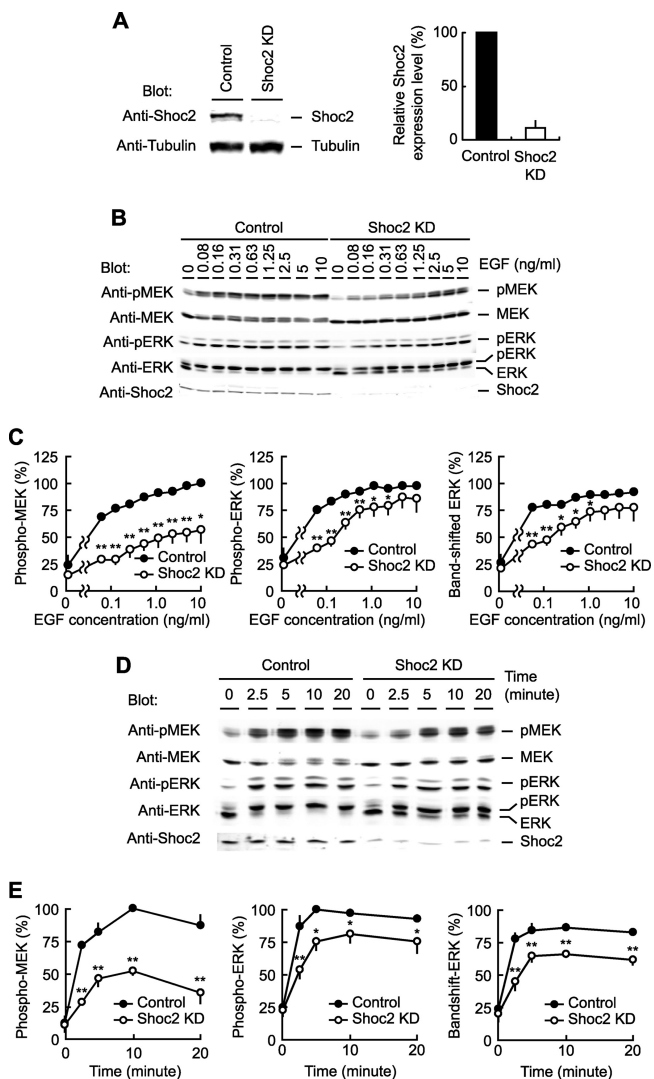


FIGURE 1. Requirement of Shoc2 for EGF-induced activation of MEK and ERK. *A*, HeLa cells were transfected with either control or Shoc2-specific siRNA. Forty-eight hours after transfection, cells were lysed and subjected to immunoblot analysis using antibodies against Shoc2 or tubulin (*left*). The relative Shoc2 expression level was quantified (*right*). *B*, HeLa cells prepared as in *A* were stimulated with EGF at the indicated concentrations for 5 min. Whole cell lysates were immunoblotted with the indicated antibodies. *C*, the experiment in *B* was repeated three times and the quantified data shown. In the *left* and *center* panels, the intensities of phospho-MEK (pMEK) and phospho-ERK (pERK) of the control cells stimulated with 10 ng/ml of EGF were set to 100%. The percentage of the slow migrating phosphorylated form of ERK is shown in the *right* panel. The average values of control cells (*closed circle*) and Shoc2 knockdown (KD) cells (*open circle*) are shown with the S.D. The symbols indicate the results of *t* test analysis; **, $p < 0.01$; *, $p < 0.05$ compared with the control. *D*, HeLa cells prepared as in *A* were stimulated with 1.0 ng/ml of EGF, and followed over the time course of MEK and ERK phosphorylation. Whole cell lysates were immunoblotted with the indicated antibodies. *E*, the experiments in *D* were repeated three times and the quantified data are shown as in *D*. The symbols indicate the results of *t* test analysis; **, $p < 0.01$; *, $p < 0.05$ compared with the control.

filters used for the dual-emission imaging studies were obtained from Omega Optical (Brattleboro, VT): an XF1071 (440AF21) excitation filter, an XF2034 (455DRLP) dichroic mirror, and two emission filters (XF3075/480AF30 for CFP and XF3079/535AF26 for FRET). After background subtraction, FRET/CFP ratio images, which were used to represent the levels of FRET, were created with MetaMorph software.

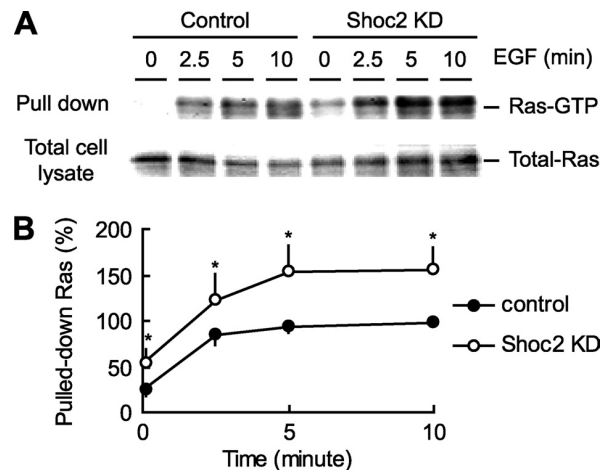


FIGURE 2. Effect of Shoc2 depletion on the activation of Ras measured by the pull-down method. *A*, control and Shoc2 knockdown (KD) cells were starved for 6–12 h, treated with 1.0 ng/ml of EGF for the indicated time periods, and then examined by pull-down assay to detect active Ras. *B*, the amount of pulled-down Ras in *A* was quantified. Experiments were repeated four times and the average fold-increases compared with the maximal value in each experiment are shown with the S.D. The symbols indicate the results of *t* test analysis; *, $p < 0.05$ compared with the control.

Calculation of Time Constants—After image processing by MetaMorph, FRET/CFP ratios were exported and analyzed by Microsoft Excel software. Time constants from just after EGF addition to the time when activation reached the maximum were calculated by fitting with the following single exponential function using the solver function in Microsoft Excel: $FRET(t) = \text{amplitude} \times [1 - \exp(-t/\tau)] + \text{basal}$, where τ indicates a time constant. The amplitude is the increase of the FRET/CFP signal after EGF stimulation, and *basal* is the basal value of FRET/CFP before EGF stimulation.

Modeling and Numerical Simulation—All kinetic reactions were described with mass action kinetics by using CellDesigner (version 4.0 β) (31). Then, the ordinary differential equations with parameters were exported to Matlab software (version R2008b; Mathworks Inc., Natick, MA) through a Systems Biology Workbench (version 2.7.8) (32). Ordinary differential equations were numerically solved by using ode23 solver of Matlab. The spatial RasGAP gradient was assumed to be a bell-shaped curve, as described previously (29), and was obtained with the following exponential function: $RasGP(x) = (A - B) \times \exp(-x_2 2\delta) + B$. The values of $A = 3$, $B = 0.36$, and $\delta = 0.1$ were used in Fig. 6A. See [supplemental figures and tables](#) for details.

RESULTS

Requirement of Shoc2 for EGF-induced Activation of MEK and ERK—To explore the role of Shoc2 in the Ras-ERK signaling cascade, we first knocked down endogenous Shoc2 with siRNA. In Shoc2 siRNA-transfected HeLa cells, the level of Shoc2 proteins was reduced to less than 10% of that in the control cells (Fig. 1A). We also confirmed the reduction of mRNA of the endogenous Shoc2 by reverse transcription-PCR analysis (data not shown).

In the HeLa cells used in our experiments, Shoc2 knockdown was found to affect the level of phospho-MEK and phospho-ERK upon stimulation, particularly at a low concentration of

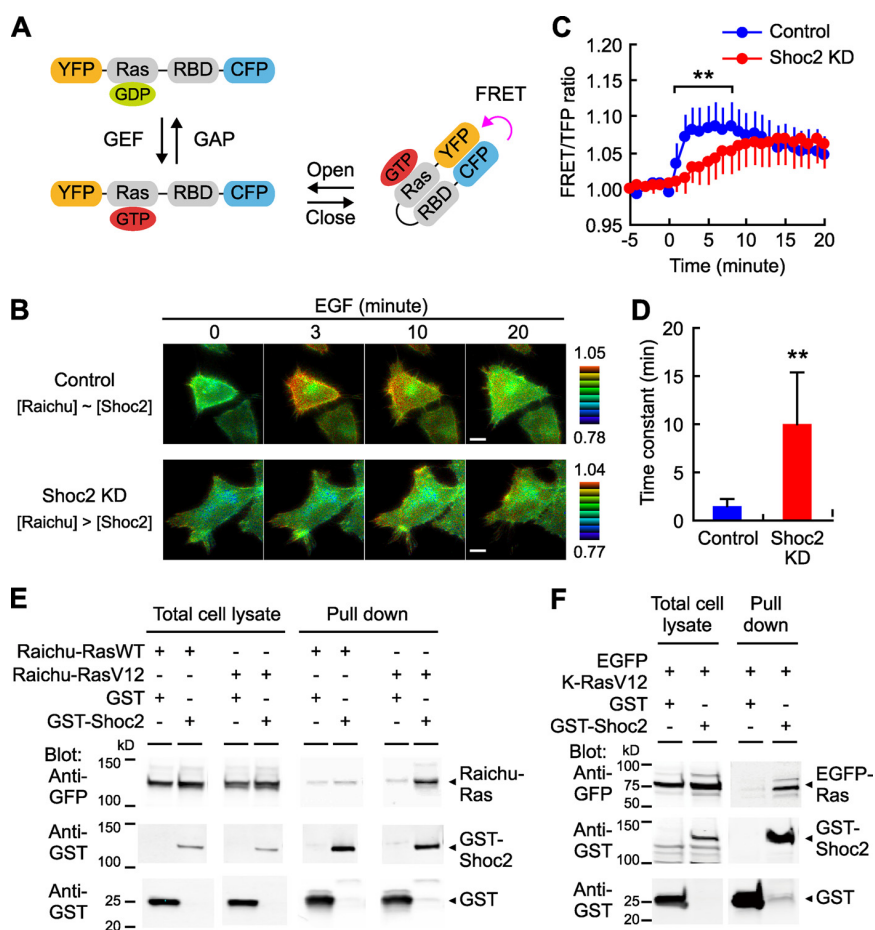


FIGURE 3. Effect of Shoc2 knockdown (KD) on the activation of Ras detected by FRET imaging. *A*, a schematic model of Raichu-Ras is shown. Within the probe, Ras is activated by GEF followed by association of Raf-RBD. *B*, HeLa cells stably expressing Raichu-Ras were transfected with control (*upper*) or Shoc2-targeted siRNA (*lower*). Two days later, the cells were starved for 6 h. Then, images were obtained every 1 min for 30 min after stimulation with 1.0 ng/ml of EGF. Representative ratio images of FRET/TFP at the indicated time points after EGF addition (in minutes) are shown in the intensity-modulated display mode. In the intensity-modulated display mode, eight colors from red to blue are used to represent the FRET/TFP ratio, with the intensity of each color indicating the mean intensity of FRET and TFP. The *upper* and *lower* limits of the ratio range are shown on the *right*. Bars, 10 μ m. *C*, the relative FRET/TFP ratios normalized by the average FRET/TFP before stimulation were plotted until 20 min after EGF addition with the S.D. The *blue* and *red* lines indicate control and Shoc2-depletion, respectively. The *symbols* indicate the results of *t* test analysis; **, $p < 0.01$ compared with the control. *D*, the *bar graph* represents the average of the time constants in control cells ($n = 32$) or that in Shoc2-knockdown cells ($n = 19$). The *symbol* shows the results of *t* test analysis; **, $p < 0.01$ compared with the control. *E*, HeLa cells were transfected with expression plasmids of Raichu-Ras-WT or Raichu-Ras-V12, and GST or GST-Shoc2. Forty-eight hours after transfection, the cells were lysed and pulled down by glutathione beads. The cell lysates (*left*) and eluates (*right*) were subjected to immunoblot analysis with antibodies against GFP and GST as indicated. Experiments were repeated three times, and the representative blots are shown. *F*, HeLa cells expressing EGFP-K-Ras-V12 and GST or GST-Shoc2 were lysed and pulled down by glutathione beads as in *E*. The cell lysates (*left*) and eluates (*right*) were subjected to immunoblot analysis with antibodies against GFP and GST as indicated. Experiments were repeated two times, and representative blots are shown.

EGF (Fig. 1, *B* and *C*). Furthermore, EGF-induced phosphorylation of MEK and ERK was suppressed with a slight delay in Shoc2-depleted cells (Fig. 1, *D* and *E*). Shoc2 depletion reproducibly inhibited the EGF-induced phosphorylation of MEK and ERK by one-quarter to one-half of the maximal activation. Thus, Shoc2 positively, but moderately, regulates EGF-induced activation of the MAP kinase signaling cascade as previously reported (33).

Effect of Shoc2 Knockdown on Ras Activity Measured by Pull-down Assay—Shoc2 was originally identified as a positive regulator of Ras-mediated signal transduction (15); therefore, we

examined the effect of Shoc2 knockdown on Ras activity by a pull-down assay with the Ras-binding domain of c-Raf (Raf-RBD). In HeLa cells, Shoc2 depletion significantly increased both the basal and EGF-stimulated levels of Ras-GTP as measured by the pull-down assay (Fig. 2). Considering the results in Fig. 1, these data suggest that Shoc2 potentiates the Raf-ERK signaling cascade at a point downstream of Ras activation. The elevation of Ras activity by Shoc2 knockdown was unexpected, but could be explained by impairment of the negative feedback loop from ERK to Sos, a guanine nucleotide exchange factor of Ras (34).⁵

Effect of Shoc2 Knockdown on Ras Activity Measured by FRET Imaging—We next investigated the mode of action of Shoc2 in Ras signaling by employing a Ras biosensor, Raichu-Ras, which is based on the principle of FRET (25). In this biosensor design (Fig. 3*A*), activated GEF converts Ras-GDP within the probe to Ras-GTP, induces intramolecular binding of Ras-GTP to the Raf-RBD, and thereby brings CFP in closer proximity to YFP, resulting in an increase in FRET from CFP to YFP.

We first established a HeLa cell line stably expressing Raichu-Ras, in which the donor fluorophore, CFP, was replaced with another cyan fluorescent protein variant, TFP (see “Experimental Procedures”). In this cell line, the intracellular concentration of the Raichu-Ras biosensor was about 1.0 μ M,⁵ which is close to the concentration of endogenous Ras proteins, 0.40 μ M (supplemental Table S1) (35). Cells expressing Raichu-Ras were excited at 440 nm and imaged with emission filters of

530 and 480 nm FRET and TFP or CFP, which yielded FRET and TFP or CFP images, respectively. The FRET/TFP or FRET/CFP ratio reflects the FRET efficiency from TFP or CFP to YFP and correlates with Ras activity (25). In the control HeLa cells, upon EGF stimulation the FRET/TFP ratio was rapidly increased in a broad area of the cell (Fig. 3*B*). Meanwhile, in Shoc2-depleted cells the FRET/TFP ratio was increased slowly in the peripheral region of the cells (Fig. 3*B*). We quantitatively

⁵ Y. Kamioka, unpublished data.

Shoc2 Regulates Ras Signaling

measured the FRET level averaged over an entire cell area at each time point and obtained the time constants ($\tau_{1/e}$) during the early phase of Ras activation by exponential approximation (Fig. 3, C and D). The time constant in knockdown cells ($\tau_{1/e} = 9.9$ min) was significantly larger than that in the control cells ($\tau_{1/e} = 1.5$ min). Because Shoc2 depletion resulted in an increase in Ras activity (Fig. 2) and a decrease in MEK and ERK phosphorylation (Fig. 1), these findings obtained by FRET imaging suggested that Shoc2 regulated the binding of Ras to Raf. Of note, the FRET/TFP ratio at 20 min was comparable between the control and Shoc2-knockdown cells.

Following this observation, we examined whether Shoc2 directly binds to Raichu-Ras by the co-precipitation method. GST-Shoc2, but not GST, pulled down Raichu-Ras-V12, in which the GTPase activity of Ras was impaired, more efficiently than the wild type Raichu-Ras (Fig. 3E). We confirmed that K-Ras-V12 was also pulled down by GST-Shoc2 (Fig. 3F). Thus, Ras in the Raichu biosensor binds to Shoc2 as did the authentic Ras in a GTP-dependent manner.

Effect of Expression of Shoc2 on Ras Activity—To gain further insight into the role of Shoc2 on Ras-Raf signaling, we next used COS7 cells, in which Raichu-Ras biosensor proteins can be overexpressed by the transient transfection method. The spatial and temporal patterns of the EGF-induced increase in FRET in control COS7 cells were virtually identical with those in Shoc2-depleted HeLa cells, *i.e.* activation of Ras was prominent at the periphery of the cells (Fig. 4A) and the time constant ($\tau_{1/e} = 12.1$ min) was markedly larger than that of the HeLa cells (Fig. 4, B and C). We reasoned that this observation was due to the relative deficiency of Shoc2 protein compared with the overexpressed Raichu-Ras biosensor. In agreement with this assumption, overexpression of Shoc2 was found to increase the population of cells, showing a rapid and widespread activation pattern (Fig. 4B). Accordingly, the time constants were significantly decreased in Shoc2-expressing COS7 cells ($\tau_{1/e} = 6.3$ min).

Numerical Simulation of the Effect of Shoc2 on the Ras FRET Biosensor—To dissect the molecular mechanism underlying Shoc2-mediated acceleration and enhancement of Ras signaling, we developed kinetic models for the action of Shoc2 and Raichu-Ras as follows. First, we included Raichu-Ras in the Ras-ERK cascade model that was previously built with experimentally determined parameters (35) (supplemental Tables S1 and S2). Second, the parameters affecting Raichu-Ras were constrained by the time constant in the absence of Shoc2 as observed in Fig. 3 ($1/(k_{\text{open}} + k_{\text{close}}) = \tau_{1/e} = 10$ min) (supplemental Table S2). Finally, we developed two possible models that could account for the roles of Shoc2. Notably, we assumed that Shoc2 activity is up-regulated upon EGF stimulation (supplemental Figs. S1 and S2), because we did not detect remarkable inhibition of MEK and ERK by the Shoc2 knockdown (Fig. 1, D and E).

In the first model, which we named the Shoc2 stabilizer model, we assumed that Shoc2 stabilizes the complex formed between Ras-GTP and Raf-RBD to prolong the lifetime of the complex (Fig. 5A and supplemental Fig. S1 and Table S2). This model includes two variables related to Shoc2, the Shoc2 concentration and the dissociation constant ($K_d = k_d/k_a$) of the

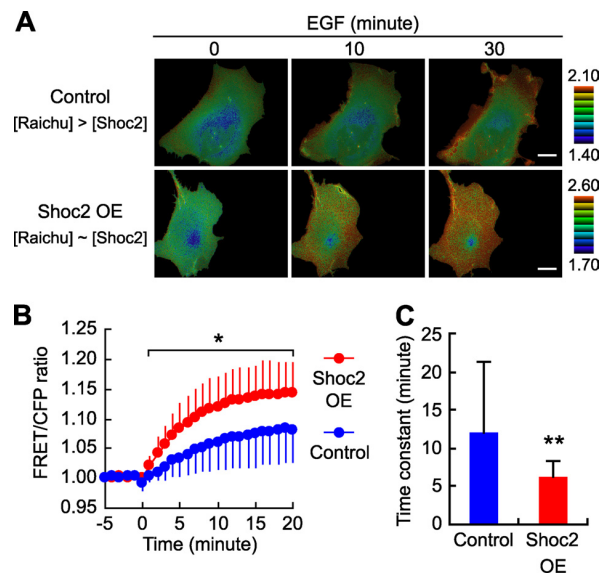


FIGURE 4. Effect of Shoc2 expression on the activation of Ras in COS7 cells. A, COS7 cells were transfected with pRaichu-Ras and with control (upper) or Shoc2-expression plasmid (lower, Shoc2 overexpression; Shoc2 OE). Images were obtained every 1 min for 30 min after stimulation with 25 ng/ml of EGF. Representative ratio images of FRET/CFP are shown at the indicated time points after EGF addition. Bars, 20 μm . B, the relative FRET/CFP ratios of the cells were obtained as described in the legend to Fig. 2B and plotted until 20 min after EGF stimulation with the S.D. The blue and red lines indicate control and Shoc2 expression, respectively. The symbol indicates the results of t test analysis; *, $p < 0.05$ compared with the control. C, the bar graph represents the average of the time constants in control cells ($n = 15$) or that in Shoc2-expressing cells ($n = 23$). The symbol shows the results of t test analysis; **, $p < 0.01$ compared with the control.

binding of Shoc2 to the Ras-Raf complex in the Raichu-Ras biosensor (Fig. 5A). The Shoc2 concentration in HeLa cells was measured by quantitative immunoblotting and was 0.67 μM (supplemental Table S1).⁵ Varying the Shoc2 concentration from 0 to 0.67 μM and K_d from 0 to 1.0 μM , we failed to reproduce the rapid and transient increase in the amount of Ras-Raf complex (Fig. 5, C and D), which should have been similar to the temporal pattern of the input EGFR phosphorylation (Fig. 5B). Hence, we excluded this model.

The critical observation for understanding the role of Shoc2 may be that Shoc2 significantly accelerated the kinetics of Ras-Raf complex formation as measured with the Raichu-Ras biosensor (Figs. 3 and 4). To reproduce this observation, in the second model we assumed that Ras-GTP first binds to Shoc2 and subsequently to Raf (Fig. 5E and supplemental Fig. S2 and Table S2). The key concept of this model is that Shoc2 accelerates the kinetics of both association and dissociation of Ras-GTP and Raf; therefore, we named this model the Shoc2 accelerator model. Because the expression of Shoc2 alone did not increase the amount of Ras-Raf complex in steady state, we set the ratio of association to dissociation rate of the Ras-Raf binding to be constant, that is to say, $k^{\text{open}}/k^{\text{close}}$ in the presence of Shoc2 = $k_{\text{open}}/k_{\text{close}}$ in the absence of Shoc2 (Fig. 5E and supplemental Table S2). For further analysis, we defined the acceleration factor (AF) as $k^{\text{open}}/k^{\text{open}} = k^{\text{close}}/k^{\text{close}}$, which represents the acceleration of both association and dissociation of the Ras-Raf binding (Fig. 5E and supplemental Table S2) (see "Discussion"). With this Shoc2 accelerator model, we were able

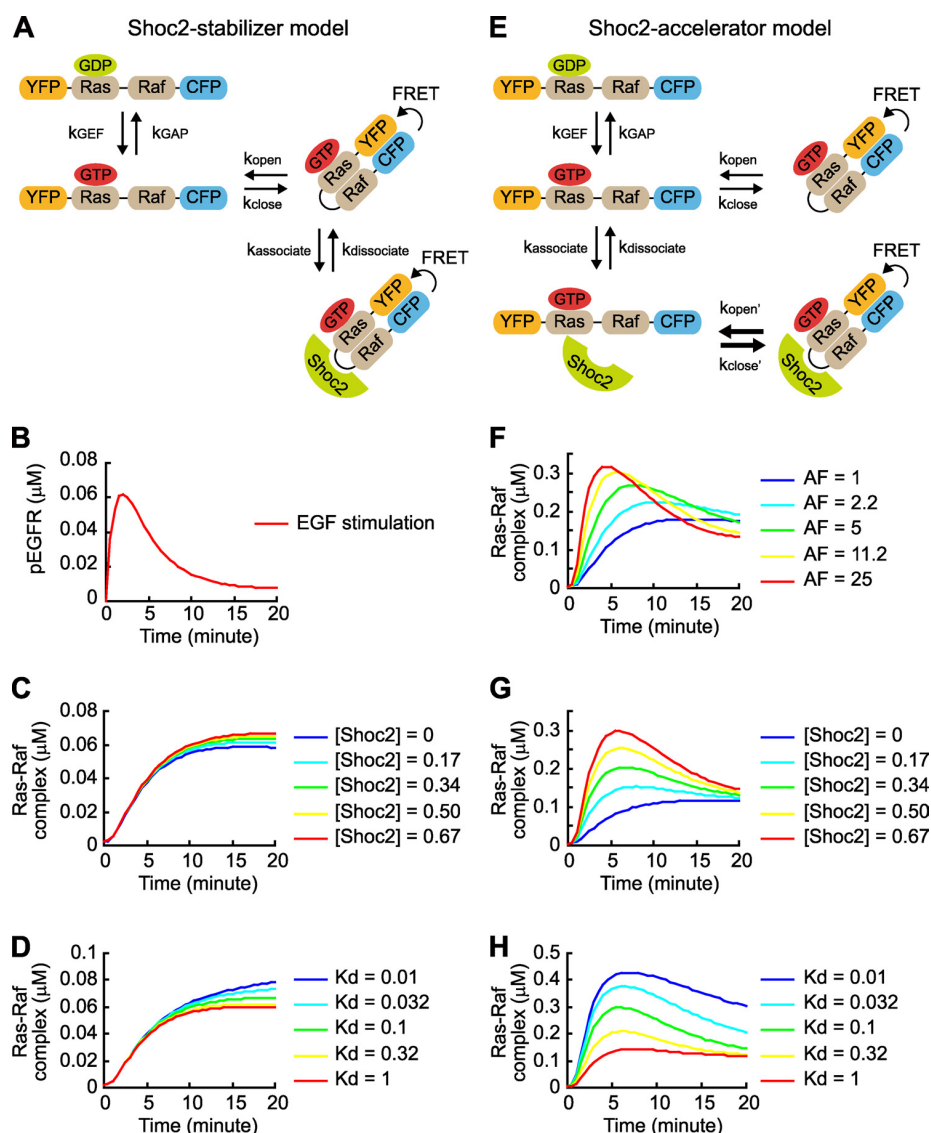


FIGURE 5. Numerical simulation of the effect of Shoc2 on the Ras-Raf complex formation. *A*, a schematic view of the Shoc2 stabilizer model. In this model, Shoc2 binds to and stabilizes the complex of Ras and Raf (supplemental Fig. S1 and Tables S1 and S2). *B–D*, results of numerical simulation of the Shoc2 stabilizer model with varying Shoc2 concentrations or dissociation constant (K_d) of the Shoc2 from Ras-GTP in the Raichu-Ras biosensor. The default values of the Shoc2 concentration and K_d were $0.67 \mu\text{M}$, which is equal to the physiological concentration, and $0.1 \mu\text{M}$, respectively. The amount of the Ras-Raf complex correlates with the experimentally obtained FRET/TFP or FRET/CFP values shown in Figs. 3 and 4. *E*, a schematic view of the Shoc2 accelerator model. In this model, Shoc2 binds to Ras-GTP and accelerates the opening and closing of the Raichu-Ras biosensor (supplemental Fig. S2). *F–H*, results of numerical simulation of the Shoc2 accelerator model with varying Shoc2 concentration, K_d , and AF. Here, AF is defined as follows: $\text{AF} = k^{\text{open}}/k^{\text{close}} = k^{\text{close}}/k^{\text{close}}$. The default values of Shoc2 concentration, K_d , and acceleration factor were $0.67 \mu\text{M}$, $0.1 \mu\text{M}$, and 5.0, respectively.

to recapitulate the Shoc2-mediated enhancement and acceleration of Ras-Raf complex formation upon stimulation ($\tau_{1/e} = 1.8 \text{ min}$), when AF was set to more than 5.0 (Fig. 5*F*) and the Shoc2 concentration was set to the near endogenous level (Fig. 5*G*). Notably, this effect of Shoc2 was highly dependent on the dissociation constant (K_d) of the binding of Shoc2 and the Ras-Raf complex (Fig. 5*H*).

Simulation of Shoc2-mediated Spatio-Temporal Activation of the Ras FRET Biosensor—We next investigated whether the Shoc2 accelerator model could account for the effect of Shoc2 on widespread Ras-Raf complex formation, as experimentally

shown in Figs. 3 and 4. We previously reported that in COS7 cells the spatial gradient of RasGAP activity, high at the center and low at the periphery of the cells, predominantly determines the spatial pattern of Ras activity (29). We input this spatial pattern of RasGAP activity into the current Shoc2 accelerator model (Fig. 6*A*) and examined the effect of Shoc2 knockdown on the spatial gradient of Ras activity. We found that the accelerator model reasonably reproduced the spatial distribution of the Ras-Raf complex shown in Figs. 3 and 4. Namely, in the presence of Shoc2 proteins the FRET signal of Raichu-Ras increased rapidly and diffusely upon stimulation (Fig. 6*B*), and in the absence of Shoc2, the increase of the FRET signal was delayed and restricted at the periphery of the cell (Fig. 6*C*). This analysis suggested that not only the distribution of RasGAPs but also the level of Shoc2 determines the spatial pattern of Ras activation.

Simulation of the Effect of Shoc2 on EGF-induced Ras and ERK Activation—Finally, we examined the contribution of Shoc2 to the Ras-ERK signaling cascade in the Shoc2 accelerator model. Knockdown of the Shoc2 protein did not affect the amount of Ras-GTP to a detectable level (Fig. 7*A*). This observation *in silico* is against the one *in cellulo* (Fig. 2). This discrepancy is probably due to the lack of the negative feedback loop from ERK to Sos in the present simulation model; however, this issue is beyond the scope of this study. Meanwhile, Shoc2 knockdown reproduced the decrease of EGF-induced Ras-Raf complex formation, and this effect was most obvious between 0 and 5 min after stimulation (Fig. 7*B*). Accordingly, Shoc2 knockdown decreased the initial velocities and maximum levels of EGF-induced phosphorylation of MEK and ERK (Fig. 7, *C* and *D*), which was consistent with the experimental observations (Fig. 1*E*). In conclusion, the Shoc2 accelerator model adequately explains the observed effect of Shoc2 knockdown.

DISCUSSION

Previous studies have indicated that Shoc2 functions as a scaffold for Ras-Raf signaling (17, 18); however, the mode of

Shoc2 Regulates Ras Signaling

action of Shoc2 is not understood clearly. Here, based on an analysis combining FRET imaging and computer-assisted kinetic simulation, we suggest that Shoc2 plays primarily two roles in EGF-induced ERK activation (Fig. 8). First, Shoc2 reserves Ras-GTP for Raf. Second, Shoc2 accelerates Ras-GTP binding to Raf, enabling a rapid temporal response to growth factor stimulation. The reservoir and accelerator

functions are typically manifested by the increase in the level and velocity of activation of ERK, respectively (Fig. 7D).

The accelerator function of Shoc2 enables this protein to transmit the temporal pattern of EGFR activity faithfully to the Raf activity. In other words, without Shoc2, the slow Ras-Raf binding process functions as a low-pass filter in the EGFR-Ras-ERK signaling cascade. In addition to the acceleration of Ras-Raf signaling temporally, Shoc2 also regulates Ras activity spatially within the EGF-stimulated cells. We have shown previously that the Ras activation level is higher in the region close to the cell edge and decreased gradually toward the center of the cells (25) (see also Figs. 3 and 4) and that this spatial gradient of Ras activity is mainly caused by a gradient in GAP activity, rather than GEF activity (29). Shoc2 protein binds to free Ras-GTP and desensitizes it for RasGAP accessibility; therefore, Shoc2 functions to attenuate the spatial gradient of Ras-Raf signaling as shown in Figs. 3 and 4.

How does Shoc2 serve as the accelerator in Ras-Raf binding? Because Shoc2 binds both Ras-GTP and Raf and provides a second binding site for Raf in the Ras-Shoc2 complex, the increase in the association rate is reasonable. At the same time, we speculate that Shoc2 binding increases the dissociation rate of Raf from Ras. Because Shoc2 binds to Ras-GTP, but not Ras-GDP (17), and because the conformational change of Ras upon GTP/GDP exchange is limited to a small portion of the Switch I and II regions (36), it is reasonable to speculate that Shoc2 binding affects the dissociation rate of the Raf-Ras complex. Alternatively, acceleration of the reaction rates might be partly explained by the phenomenon reported as "substrate channeling," "kinetic channeling," or "metabolic channeling." In several multienzyme complexes, reaction rates can be increased due to the direct transfer of substrates inside the multienzyme complex, without diffusion of the substrates from the enzyme complex (37–39). We envisage that this scheme holds for the association/dissociation of Ras and Raf on the surface of Shoc2. Because Ras, Raf, and the Ras-Raf complex are restrained in a comparatively narrower space in this scenario, their effective concentrations will be increased, resulting in acceleration of the

association/dissociation reactions (see reaction 28 in [supplemental Table S2](#) for the implementation in detail). In this sense, AF can be interpreted as the thermodynamic activity coefficient converting apparent concentrations of Ras, Raf, and the Ras-Raf complex into their local effective concentrations. So far we have failed to obtain a sufficient amount of recombinant Raf proteins to test these hypotheses *in vitro*, but we are currently attempting to develop a FRET-based method to measure the dissociation rate in living cells.

It is worth noting the discrepancies between the two assays for Ras activities: the pull-down assay with GST-Raf-RBD and the FRET imag-

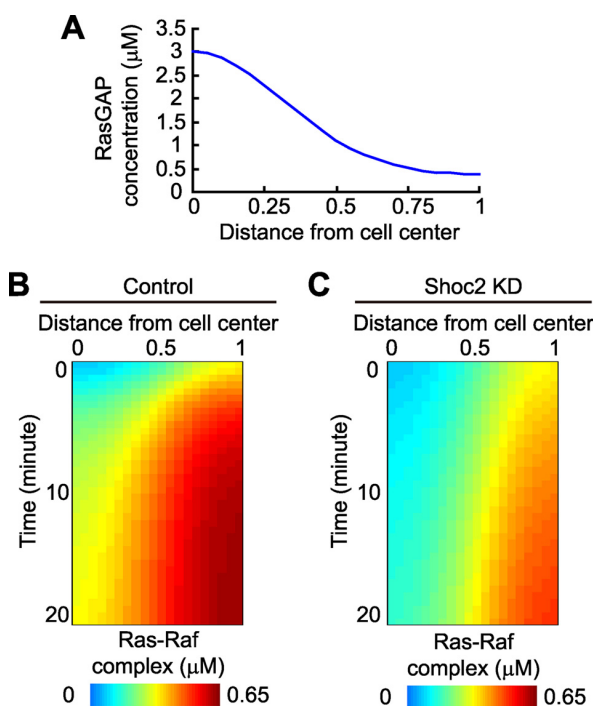


FIGURE 6. Effect of Shoc2 knockdown (KD) on the spatial gradient of Ras-Raf complex formation. A, the intracellular spatial gradient of the RasGAP concentration is derived from a previous report (29). B and C, the concentrations of the Ras-Raf complex, which are equivalent to the closed form of Raichu-Ras, were numerically solved in control (B) and Shoc2-depleted cells (C), and shown as a heat map. All kinetic reactions are the same as in Fig. 5E except for the RasGAP concentration.

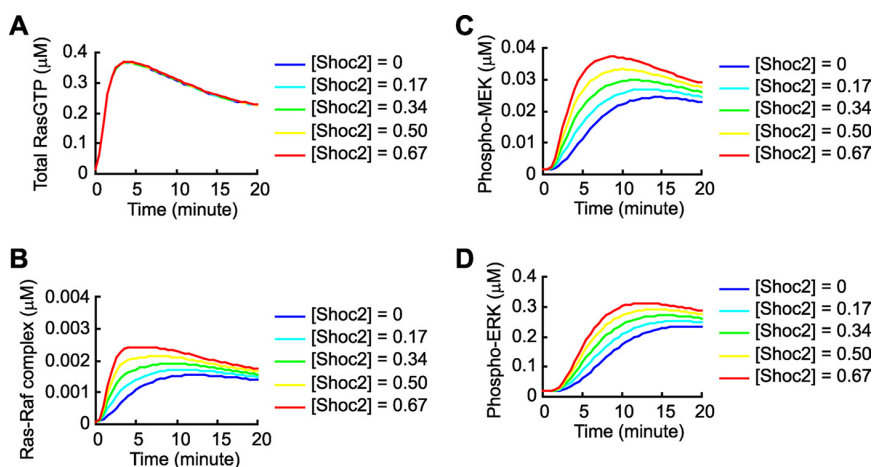


FIGURE 7. Verification of the effect of Shoc2 on EGF-induced activation of Ras and ERK. The kinetic model used in Fig. 5E is integrated with our previous Ras/ERK MAP kinase model (see "Results"). All kinetic reactions and parameters are described in [supplemental Fig. S2 and Tables S1 and S2](#). A–D, results of computational simulation for total Ras-GTP (A), Raf-bound Ras-GTP (B), phosphorylated MEK (C), and phosphorylated ERK (D) are shown. Shoc2 concentration was varied as indicated.

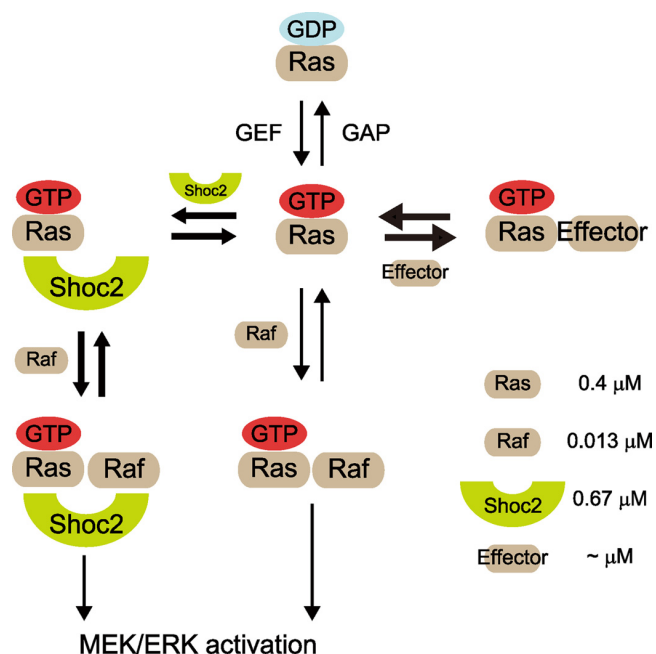


FIGURE 8. A schematic view of Shoc2 function. In this Shoc2 accelerator model, Shoc2 reserves Ras-GTP for Raf and accelerates Ras-GTP binding to Raf.

ing with Raichu-Ras (Figs. 2–4). In the former case, GST-Raf-RBD binds to and pulls down free Ras-GTP. This method can provide direct information on the change in the free Ras-GTP level; however, it does not provide information on Ras-GDP (40). Meanwhile, in the latter method, the Raichu-Ras biosensor monitors the intracellular balance of the activities of GEFs and GAPs for Ras in living cells (41). The conformational change of Raichu-Ras during activation consists of two steps: a GDP/GTP exchange reaction on Ras and Ras-GTP binding to Raf-RBD. Similarly, the inactivation process consists of GTP hydrolysis and dissociation of the Ras-Raf complex. Therefore, the FRET level used as the output is affected not only by the level of GTP/GDP on Ras, but also by the rate of Ras-Raf binding. We took advantage of this property of the Raichu-Ras biosensor to study the molecular mechanism by which Shoc2 enhances Ras-Raf signaling. This property also provided a potential disadvantage of Raichu-Ras. In principle, Raichu serves as an inhibitor of Ras-Raf signaling by competing with endogenous Ras for Shoc2. Our rationale for the use of Raichu is that Raichu would not remarkably interfere with the signaling as far as its expression level is comparable with that of the endogenous proteins. In fact, this is the reason why we established HeLa cell lines, in which the Raichu-Ras biosensor was expressed at a level comparable with the endogenous Ras (Fig. 3). If Raichu-Ras sequesters Shoc2 and inhibits ERK activation, the activation of Raichu-Ras should prolong due to the insufficient negative feedback loop to Sos. But, the steady-state level of activated Raichu-Ras in the later phase (10–30 min) was at a similar level between the control and Shoc2-depleted HeLa cells (Fig. 3B), indicating that the perturbation caused by the Raichu-Ras biosensor is negligible at least in this cell line.

In conclusion, we propose a novel role of Shoc2 in the Ras/ERK MAP kinase signaling cascade. Our results may define

Shoc2 as a spatial and temporal amplifier of the specific pathway from Ras to Raf, acting via an interaction of Ras-GTP with Shoc2 prior to binding to Raf, and simultaneously protecting inactivation of Ras by GAP. The function and regulation of scaffold proteins are complicated, and a detailed understanding of their mechanisms will require the use of new experimental tools, such as mathematical modeling and fluorescent imaging, in addition to classic biochemical approaches. Further characterization of the regulation of Shoc2 with negative feedback loop(s) will be added in the future.

Acknowledgments—We thank M. White, A. Miyawaki, T. Akagi, and J. Miyawaki for plasmids. We also thank A. Nishiyama-Abe and Y. Kasakawa for technical assistance. We are grateful to members of the Matsuda Laboratory for helpful input.

REFERENCES

1. Sturgill, T. W., and Wu, J. (1991) *Biochim. Biophys. Acta* **1092**, 350–357
2. Lewis, T. S., Shapiro, P. S., and Ahn, N. G. (1998) *Adv. Cancer Res.* **74**, 49–139
3. Nishida, E., and Gotoh, Y. (1993) *Trends Biochem. Sci.* **18**, 128–131
4. Chang, L., and Karin, M. (2001) *Nature* **410**, 37–40
5. Pearson, G., Robinson, F., Beers Gibson, T., Xu, B. E., Karandikar, M., Berman, K., and Cobb, M. H. (2001) *Endocr. Rev.* **22**, 153–183
6. Barbacid, M. (1987) *Annu. Rev. Biochem.* **56**, 779–827
7. Bos, J. L. (1989) *Cancer Res.* **49**, 4682–4689
8. Lowy, D. R., and Willumsen, B. M. (1993) *Annu. Rev. Biochem.* **62**, 851–891
9. Takai, Y., Sasaki, T., and Matozaki, T. (2001) *Physiol. Rev.* **81**, 153–208
10. Kolch, W. (2005) *Nat. Rev. Mol. Cell Biol.* **6**, 827–837
11. Shaw, A. S., and Filbert, E. L. (2009) *Nat. Rev. Immunol.* **9**, 47–56
12. Levchenko, A., Bruck, J., and Sternberg, P. W. (2000) *Proc. Natl. Acad. Sci. U.S.A.* **97**, 5818–5823
13. Bashor, C. J., Helman, N. C., Yan, S., and Lim, W. A. (2008) *Science* **319**, 1539–1543
14. Morrison, D. K., and Davis, R. J. (2003) *Annu. Rev. Cell Dev. Biol.* **19**, 91–118
15. Sieburth, D. S., Sun, Q., and Han, M. (1998) *Cell* **94**, 119–130
16. Selfors, L. M., Schutzman, J. L., Borland, C. Z., and Stern, M. J. (1998) *Proc. Natl. Acad. Sci. U.S.A.* **95**, 6903–6908
17. Li, W., Han, M., and Guan, K. L. (2000) *Genes Dev.* **14**, 895–900
18. Dai, P., Xiong, W. C., and Mei, L. (2006) *J. Biol. Chem.* **281**, 927–933
19. Rodriguez-Viciano, P., Oses-Prieto, J., Burlingame, A., Fried, M., and McCormick, F. (2006) *Mol. Cell* **22**, 217–230
20. Pollok, B. A., and Heim, R. (1999) *Trends Cell Biol.* **9**, 57–60
21. Miyawaki, A., and Tsien, R. Y. (2000) *Methods Enzymol.* **327**, 472–500
22. Kiyokawa, E., Hara, S., Nakamura, T., and Matsuda, M. (2006) *Cancer Sci.* **97**, 8–15
23. Aoki, K., Nakamura, T., Inoue, T., Meyer, T., and Matsuda, M. (2007) *J. Cell Biol.* **177**, 817–827
24. Sasagawa, S., Ozaki, Y., Fujita, K., and Kuroda, S. (2005) *Nat. Cell Biol.* **7**, 365–373
25. Mochizuki, N., Yamashita, S., Kurokawa, K., Ohba, Y., Nagai, T., Miyawaki, A., and Matsuda, M. (2001) *Nature* **411**, 1065–1068
26. Ai, H. W., Henderson, J. N., Remington, S. J., and Campbell, R. E. (2006) *Biochem. J.* **400**, 531–540
27. Day, R. N., Booker, C. F., and Periasamy, A. (2008) *J. Biomed. Opt.* **13**, 031203
28. Akagi, T., Sasai, K., and Hanafusa, H. (2003) *Proc. Natl. Acad. Sci. U.S.A.* **100**, 13567–13572
29. Ohba, Y., Kurokawa, K., and Matsuda, M. (2003) *EMBO J.* **22**, 859–869
30. Hara, S., Kiyokawa, E., Iemura, S., Natsume, T., Wassmer, T., Cullen, P. J., Hiai, H., and Matsuda, M. (2008) *Mol. Biol. Cell* **19**, 3823–3835
31. Kitano, H., Funahashi, A., Matsuoka, Y., and Oda, K. (2005) *Nat. Biotechnol.* **23**, 961–966

Shoc2 Regulates Ras Signaling

32. Sauro, H. M., Hucka, M., Finney, A., Wellock, C., Bolouri, H., Doyle, J., and Kitano, H. (2003) *OMICS* **7**, 355–372
33. Anselmo, A. N., Bumeister, R., Thomas, J. M., and White, M. A. (2002) *J. Biol. Chem.* **277**, 5940–5943
34. Chen, D., Waters, S. B., Holt, K. H., and Pessin, J. E. (1996) *J. Biol. Chem.* **271**, 6328–6332
35. Fujioka, A., Terai, K., Itoh, R. E., Aoki, K., Nakamura, T., Kuroda, S., Nishida, E., and Matsuda, M. (2006) *J. Biol. Chem.* **281**, 8917–8926
36. McCormick, F., and Wittinghofer, A. (1996) *Curr. Opin. Biotechnol.* **7**, 449–456
37. Ovádi, J., and Saks, V. (2004) *Mol. Cell. Biochem.* **256–257**, 5–12
38. Wu, N., Tsuji, S. Y., Cane, D. E., and Khosla, C. (2001) *J. Am. Chem. Soc.* **123**, 6465–6474
39. Ishikawa, M., Tsuchiya, D., Oyama, T., Tsunaka, Y., and Morikawa, K. (2004) *EMBO J.* **23**, 2745–2754
40. de Rooij, J., and Bos, J. L. (1997) *Oncogene* **14**, 623–625
41. Aoki, K., Kiyokawa, E., Nakamura, T., and Matsuda, M. (2008) *Philos. Trans. R. Soc. Lond. B Biol. Sci.* **363**, 2143–2151